

NUCLEAR STRUCTURE  
OF PROTON-RICH  $^{20-23}\text{Mg}$  ISOTOPESMOHAMMED Y. HADI<sup>a,b</sup>, AMMAR A. AL-SA'AD<sup>a,†</sup><sup>a</sup>Department of Physics, College of Science, University of Basrah, Basrah, Iraq<sup>b</sup>Al-Qasim Green University, College of Biotechnology, Babylon, Iraq*Received 18 December 2022, accepted 2 February 2023,**published online 10 February 2023*

Large-scale shell model calculations are performed within the model spaces *sd*, *zbsm* and *psdpf*, to study the positive- and negative-parity energy levels and electromagnetic transitions in the exotic  $^{20-23}\text{Mg}$  isotopes. Core-polarization effects on reduced transition probability are introduced through the first-order perturbation theory, which allows for higher energy configurations through excitations of nucleons from core orbits to that outside model space up to  $9\hbar\omega$ . The core-polarization effects have improved the agreement of  $B(E2)$  with their corresponding experimental data, and have an ignorable effect on  $B(M1)$  and  $B(E1)$ .

DOI:10.5506/APhysPolB.54.1-A3

## 1. Introduction

The stable nuclides of magnesium ( $^{24-26}\text{Mg}$ ) are of particular interest for the nuclear shell model [1–3]. As neutron number ( $N$ ) is less than 12, the resulting Mg isotopes are far away from the  $\beta$ -stability line. These proton-rich  $^{20-23}\text{Mg}$  isotopes are of special importance for their appearance in the astrophysical reactions through the rapid proton capture processes  $^A\text{Na}(p, \gamma)^{A+1}\text{Mg}$  (where  $A = 20-22$ ) [4]. Also, the structure of  $^{20}\text{Mg}$  is important since its  $\beta$  decay  $^{20}\text{Mg}(\beta^+)^{20}\text{Na}$  is relevant to the onset of the astrophysical reaction  $^{19}\text{Ne}(p, \gamma)^{20}\text{Na}$  [5, 6]. The determination of the rates of these nuclear astrophysical reactions requires some nuclear structure information of  $^{20-23}\text{Mg}$  isotopes, such as excitation energy, spin, parity, and partial decay width (related to the reduced transition probability). Thus, providing these nuclear properties motivates the extensive theoretical and experimental works within this region.

The structure of positive parity states of  $^{20-23}\text{Mg}$  can be obtained through the distribution of 4 protons and  $0 \leq N \leq 3$  neutrons over  $2s1d$  shells (*sd*-shell model space) for each isotope, respectively. The widely used

---

<sup>†</sup> Corresponding author: [ammari1sd@yahoo.com](mailto:ammari1sd@yahoo.com)

phenomenological interactions necessary for calculating the positive-parity states in normal and exotic sd-shell nuclei are those of Wildenthal (W) [7], and Brown and Richter (USDA and USDB) [8]. Recently Magilligan and Brown [9] developed the USD interactions USDC, USDCm, USDI, and USDIm. In the derivation of the recent USD-type interactions, Magilligan and Brown [9] considered 854 states in 117 nuclei with  $8 \leq N \leq 20$  and  $8 \leq Z \leq 20$ , to be used in the data set to constrain their Hamiltonians. Al-Sammarræ *et al.* [10] studied the structure of the proton-rich  $^{21,23}\text{Mg}$  (as well as  $^{25,27}\text{Mg}$ ) within sd shells model space in the presence of the interactions USDA and SDBA. Other researchers [11–17] used the W and USDA/B interactions to interpret their measurements of  $^{20-23}\text{Mg}$  properties. The structure of the intruder negative parity states in the sd-shell nuclei requires the extension of the model space to include  $1\hbar\omega$  excitations. Diget *et al.* [18] investigated the  $\gamma$ -ray spectroscopy of  $^{21}\text{Mg}$  and compared their data with the shell model calculations using the WBP [19] interaction within psd model space truncated to  $(0+1)\hbar\omega$ . Bouhelal *et al.* [20] constructed PSDPF interaction in the full psdpf model space to describe  $1\hbar\omega$  intruder states in sd shell nuclei, and they used it to present a one-to-one level correspondence between  $^{22}\text{Ne}$  and  $^{22}\text{Mg}$  [21]. Within the PSDPF interaction, a reasonable description for the negative parity energy levels of  $^{24}\text{Mg}$  and their form factors due to electron scattering was obtained in a recent study [22].

The restriction of shell model calculations within a finite model space produces truncated wave functions, which in turn affected the value of the reduced matrix elements of the one-body transition operator. To compensate for the lack of wave functions due to this truncation, core-polarization effects are added either macroscopically via effective charges, or microscopically through first-order perturbation theory which admits linear combinations of one particle–one hole ( $1p-1h$ ) excitations from the core states to higher orbits outside the model space with  $n\hbar\omega$ . The electron scattering form factors for the positive parity states in  $^{24}\text{Mg}$  [23],  $^{25}\text{Mg}$  [24] and  $^{26}\text{Mg}$  [25] are very well enhanced as the microscopic core polarization effects are incorporated in the shell model calculations.

In the present work, the model spaces sd, zbme (extended zbm) and psdpf are used to study the structure of the positive- and negative-parity states in  $^{20-23}\text{Mg}$  isotopes. The recent development of Magilligan and Brown (USDC/I) [9] for the USD interaction is used in the calculation of the positive parity states, as well as USDB interaction [8]. To calculate the negative-parity states, zbme and psdpf spaces are used, and the adopted interactions are, respectively, Reehal–Wildenthal (REWILE) [26] and Warburton–Brown (WBT) [19]. In the calculation of reduced transition probability, core polarization effects are introduced such that  $1p-1h$  configurations up to  $9\hbar\omega$  are taken into account.

## 2. Theory

The reduced probability for the electromagnetic transition operator  $O_{JT}^{\varpi}$  ( $\varpi \equiv E$  or  $M$  for electric or magnetic operators) between the initial ( $i$ ) and final ( $f$ ) nuclear states of spin and isospin  $\Gamma_i \equiv J_i T_i$  and  $\Gamma_f \equiv J_f T_f$ , respectively, is given by (Ref. [27], Eqs. (4.37) and (4.38) at the photon point)

$$B(\varpi J; i \rightarrow f) = \frac{1}{2J_i + 1} \left| \sum_{T=0,1} (-1)^{T_f - T_Z} \begin{pmatrix} T_f & T & T_i \\ -T_Z & 0 & T_Z \end{pmatrix} (\Gamma_f ||| O_{\Gamma}^{\varpi} ||| \Gamma_f) \right|^2, \quad (1)$$

where  $\begin{pmatrix} \cdot & \cdot & \cdot \\ \cdot & \cdot & \cdot \\ \cdot & \cdot & \cdot \end{pmatrix}$  is the 3j-symbol.  $T_{iZ} = T_{fZ} = T_Z = (Z - N)/2$ , and  $\Gamma \equiv JT$ . The triple-bar matrix element is used to indicate the reduction in spin and isospin spaces. The reduced many-particle matrix elements are written in terms of reduced single-particle one, as [28]

$$(\Gamma_f ||| O_{\Gamma}^{\varpi} ||| \Gamma_f) = \sum_{\alpha\beta} \text{OBDM}(\alpha, \beta, \Gamma_f, \Gamma_i, \Gamma) (\alpha ||| O_{\Gamma}^{\varpi} ||| \beta), \quad (2)$$

where  $\alpha$  and  $\beta$  denote the quantum numbers of single-particle states (including isospin), and the One-Body Density Matrix elements (OBDM) are defined by [28]

$$\text{OBDM}(\alpha, \beta, \Gamma_f, \Gamma_i, \Gamma) = \frac{\langle \Gamma_f ||| [a_{\alpha}^{\dagger} \times \tilde{a}_{\beta}] ||| \Gamma_i \rangle}{\sqrt{2\Gamma + 1}}. \quad (3)$$

The inclusion of core-polarization effects on the one-body transition operator, through first-order perturbation theory, in the presence of the residual interaction  $V_{\text{res}}$  will separate the reduced single-particle matrix elements into three parts [28]

$$\begin{aligned} (\alpha ||| O_{\Gamma}^{\varpi} ||| \beta) &= \langle \alpha ||| O_{\Gamma}^{\varpi} ||| \beta \rangle + \langle \alpha | \left| \left| O_{\Gamma}^{\varpi} \frac{Q}{E_i - H_o} V_{\text{res}} \right| \right| | \beta \rangle \\ &+ \langle \alpha | \left| \left| V_{\text{res}} \frac{Q}{E_i - H_o} O_{\Gamma}^{\varpi} \right| \right| | \beta \rangle \end{aligned} \quad (4)$$

the operator  $Q$  is the projection operator onto the space outside the model space.  $E_{i,f}$  are the initial and final states energies. The first term is due to model space, while the second and third terms are due to core-polarization effects. The core-polarization terms can be evaluated in terms of the matrix elements of residual interaction and the transition operator by introducing intermediate particle  $|\alpha_1\rangle$  and hole  $|\alpha_2\rangle$  states, and using some Racah algebra [28]

$$\begin{aligned}
& \sum_{\alpha_1 \alpha_2 \Gamma'} \frac{(-1)^{\beta + \alpha_2 + \Gamma'}}{e_\beta - e_\alpha - e_{\alpha_1} + e_{\alpha_2}} (2\Gamma' + 1) \left\{ \begin{array}{ccc} \alpha & \beta & \Gamma \\ \alpha_2 & \alpha_1 & \Gamma' \end{array} \right\} \\
& \times \sqrt{(1 + \delta_{\alpha_1 \alpha})(1 + \delta_{\alpha_2 \beta})} \times \langle \alpha \alpha_1 | V_{\text{res}} | \beta \alpha_2 \rangle \langle \alpha_2 | \| O_{\Gamma'}^{\overline{\sigma}} \| | \alpha_1 \rangle \\
& - \sum_{\alpha_1 \alpha_2 \Gamma'} \frac{(-1)^{\beta + \alpha_1 + \Gamma'}}{e_\beta - e_\alpha - e_{\alpha_2} + e_{\alpha_1}} (2\Gamma' + 1) \left\{ \begin{array}{ccc} \alpha & \beta & \Gamma \\ \alpha_1 & \alpha_2 & \Gamma' \end{array} \right\} \\
& \times \sqrt{(1 + \delta_{\alpha_2 \alpha})(1 + \delta_{\alpha_1 \beta})} \times \langle \alpha \alpha_2 | V_{\text{res}} | \beta \alpha_1 \rangle \langle \alpha_1 | \| O_{\Gamma'}^{\overline{\sigma}} \| | \alpha_2 \rangle. \quad (5)
\end{aligned}$$

The triple-bar single-particle matrix elements are written in terms of double-bar one, by [28]

$$\langle \alpha_2 | \| O_{\Gamma'}^{\overline{\sigma}} \| | \alpha_2 \rangle = \sqrt{\frac{2T+1}{2}} \sum_{t_z} P_T(t_z) \langle \alpha_2 | \| O_{j_{t_z}}^{\overline{\sigma}} \| | \alpha_2 \rangle \quad (6)$$

with

$$P_T(t_z) = \begin{cases} 1 & \text{for } T = 0, \\ (-1)^{1/2 - t_z} & \text{for } T = 1, \end{cases}$$

where  $T$  denotes the isospin,  $t_z = 1/2$  for a proton and  $-1/2$  for a neutron.

The single-particle energies in the denominator of Eq. (5) are calculated by [28]

$$e_{nlj} = \left( 2n + l - \frac{1}{2} \right) \hbar\omega + \begin{cases} -\frac{1}{2}(l+1) \langle f(r) \rangle_{nl} & \text{for } j = l - 1/2, \\ \frac{1}{2} l \langle f(r) \rangle_{nl} & \text{for } j = l + 1/2, \end{cases} \quad (7)$$

with

$$\langle f(r) \rangle_{nl} = -20A^{-2/3} \quad \text{and} \quad \hbar\omega = 45A^{-1/3} - 25A^{-2/3}.$$

The reduced matrix elements of the electric and magnetic operators are given, respectively, by [29]

$$\begin{aligned}
\langle a | \| O_J^E \| | b \rangle &= (-1)^{j_b + J - 1/2} \left\{ \frac{1 + (-1)^{l_a + l_b + J}}{2} \right\} \sqrt{\frac{(2J+1)(2j_a+1)(2j_b+1)}{4\pi}} \\
&\times \begin{pmatrix} j_a & j_b & J \\ 1/2 & -1/2 & 0 \end{pmatrix} \langle n_a l_a | r^J | n_b l_b \rangle, \quad (8)
\end{aligned}$$

and

$$\begin{aligned}
\langle a || O_J^M || b \rangle &= (-1)^{j_b+J-1/2} \left\{ \frac{1 - (-1)^{l_a+l_b+J}}{2} \right\} \sqrt{\frac{(2J+1)(2j_a+1)(2J_b+1)}{4\pi}} \\
&\times \begin{pmatrix} j_a & j_b & J \\ 1/2 & -1/2 & 0 \end{pmatrix} (J-k) \left[ g_l \left( 1 + \frac{k}{J+1} \right) - \frac{1}{2} g_s \right] \\
&\times \langle n_a l_a | r^{J-1} | n_b l_b \rangle, \tag{9}
\end{aligned}$$

with

$$k = (-1)^{l_a+j_a+\frac{1}{2}} \left( j_a + \frac{1}{2} \right) + (-1)^{l_b+j_b+\frac{1}{2}} \left( j_b + \frac{1}{2} \right),$$

where the  $g$ -factors of the proton and the neutron are respectively,  $g_l^p = 1$ ,  $g_s^p = 5.5857$ ,  $g_l^n = 0$ ,  $g_s^n = -3.8263$ . and the radial integral involving harmonic oscillator radial wave functions  $R_{nl}(r)$  are defined as

$$\langle n_a l_a | r^\lambda | n_b l_b \rangle = \int_0^\infty R_{n_a l_a}(r) r^\lambda R_{n_b l_b}(r) r^2 dr. \tag{10}$$

The adopted residual interaction is the Modified Surface Delta Interaction (MSDI) with the parameters [28]:  $A_0 \approx A_1 \approx B \approx \frac{25}{A}$  [MeV], and  $C \approx 0$ , where  $A$  is the atomic mass.

### 3. Results and discussion

We have performed the large-scale shell model calculations for the proton-rich  $^{20-23}\text{Mg}$  within the model spaces  $sd$ ,  $zbme$  ( $1p_{1/2} + 2s_{1d}$ ), and  $psdpf$ , by using OXBASH code [30]. The inert cores of these model spaces are, respectively,  $^{16}\text{O}$ ,  $^{12}\text{C}$ , and  $^4\text{He}$ . The positive parity states of  $^{20-23}\text{Mg}$  are calculated within  $0\hbar\omega$  configurations of  $sd$  and  $psdpf$  model spaces. The adopted interactions for  $sd$  space are USDB, USDC, USDI, and for  $psdpf$  space is WBT interaction. The  $0\hbar\omega$  configurations within  $psdpf$  space are obtained from the distribution of nucleons within  $sd$  shells, where the  $sd$  part of the WBT interaction is Wildenthal (W) interaction as used by Warburton and Brown [19]. Since  $zbme$  space allows for up to 4 nucleons to jump from  $1p_{1/2}$  orbit to  $1d_{5/2}$ ,  $2s_{1/2}$ , and  $1d_{3/2}$  orbits, the positive-parity states are obtained through partial  $(0+2+4)\hbar\omega$  configurations, in the presence of REWILE interaction. For the negative-parity states, two model spaces are considered,  $zbme$  and  $psdpf$ . For  $psdpf$  space, the complete  $1\hbar\omega$  configurations are made from all allowed excitations of one nucleon from  $1p$  to  $2s_{1d}$  shells or the excitation of one nucleon from  $2s_{1d}$  to  $2p_{1f}$  shells. In the OXBASH code, the WBT interaction within  $psdpf$  model space is performed by using the restriction  $(0+1)\hbar\omega$  on the space  $spsdpf$ . On the other side, the negative-parity states are made in  $zbme$  space through partial  $(0+3)\hbar\omega$  configurations.

Also, the OXBASH code is used to generate One-Body Density Matrix elements (OBDMs) which are important in the calculations of the reduced transition probabilities between nuclear shell model states. In the calculation of  $B(EJ)$  and  $B(MJ)$ , core-polarization effects are introduced through the microscopic theory that includes excitations of nucleons from the core orbits (of each model space) into higher shells up to  $9\hbar\omega$  excitations outside model space, with  $\hbar\omega = 45A^{(-1/3)} - 25A^{(-2/3)}$ . The core orbits are  $1s$  and  $1p$  for sd model space,  $1s_{1/2}$  and  $1p_{3/2}$  for zbm model space and  $1s_{1/2}$  for psdpf model space. The results of  $B(\varpi J)$  that are calculated within model space are denoted as MS, while incorporated core-polarization effects are denoted as MS+CP.

### 3.1. $^{20}\text{Mg}$ isotope

In sd shell model space, the levels of  $^{20}\text{Mg}$  are extracted from the configurations interaction of the distribution of 4 protons among  $1d_{5/2}$ ,  $2s_{1/2}$ , and  $1d_{3/2}$  harmonic oscillator orbits. The interactions were, USDB, USDC, and USDI. The results very well reproduce the ground state and the first excited state as shown in Fig. 1. Experimentally, there is an energy level at 3.7 MeV with a tentative assignment  $(2^+, 4^+)$ , and an unassigned  $J^\pi$  value level at 5.37 MeV. The doublet state  $(2^+, 4^+)$  has appeared in previous calculations that were performed in the framework of cluster model [31], shell model within  $sd f_{7/2} p_{3/2}$  space in the presence of  $NN + 3N$  force [32], and Gamow shell model [33]. In the present calculations, the  $(2^+, 4^+)$  state appears clearly, where the USD-type and WBT interactions found the first  $4^+$  state around 3.7 MeV, and the second  $2^+$  state around 4.2 MeV, while the

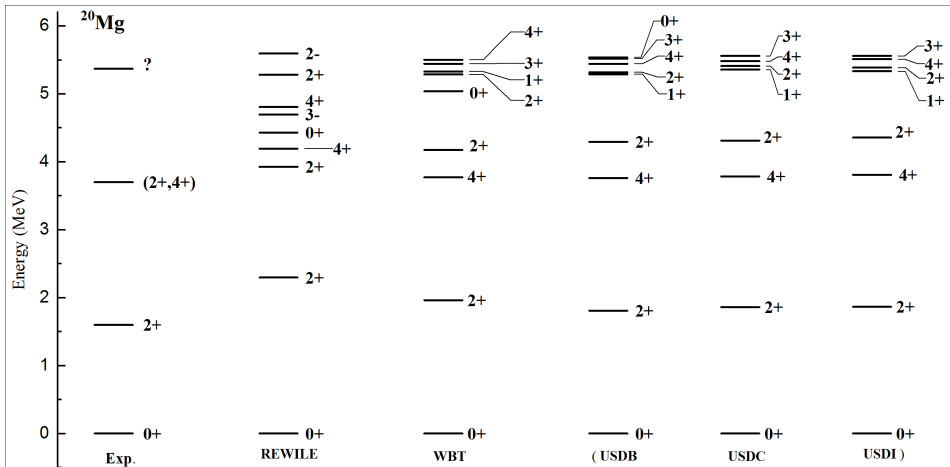


Fig. 1. The calculated and experimental level schemes for  $^{20}\text{Mg}$ . The experimental data are taken from [34].

calculations of zbme space interchanged their sequence. A third  $2^+$  state is found in all of the present calculations corresponding to the experimentally unassigned state at 5.37 MeV, however, the assignment of this state as third  $2^+$  state is not conclusive unless supported by the experiment. The zbme space calculations predict two negative-parity states below 5.5 MeV which are the  $2^-$  and  $3^-$  states.

Table 1 displays the model space (MS) calculations of the reduced transition probabilities in  $^{20}\text{Mg}$  and compares them with that included core-polarization effects (MS+CP). The effect of CP is very clear on  $B(E2)$  and  $B(E3)$ , and this effect on  $B(M1)$ ,  $B(M2)$  and  $B(E1)$  is ignorable. The experimental data for transition probabilities in  $^{20}\text{Mg}$  are not available. However, our theoretical MS+CP result for  $B(E2, 2_1^+ \rightarrow 0_1^+)$  is comparable with 9.16 W.u. calculated by Descouvemont [31] in the framework of cluster model that considered  $^{20}\text{Mg}$  as  $^{16}\text{O}+2p+2p$  clusters and interacted via Minnesota force.

Table 1. The calculated reduced transition probabilities (in W.u.) in  $^{20}\text{Mg}$ . The calculations performed within shell model space are referred as (MS) and the ones that included core polarization effects as (MS+CP).

$J_{ni}^\pi \rightarrow J_{nf}^\pi$	Exp.		zbme		sd		psdpf	$B(\varpi L)$	Other calc.
			REWILE	USDB	USDC	USDI	WBT		
$2_1^+ \rightarrow 0_1^+$	—	MS	4.801	6.355	6.369	6.409	6.158	E2	9.16 <sup>a</sup>
		MS+CP	7.083	9.378	9.398	9.958	6.158		
$3_1^- \rightarrow 0_1^+$	—	MS	1.04				2.827	E3	
		MS+CP	2.671				6.614		
$3_1^- \rightarrow 2_1^+$	—	MS	0.432				1.844	E3	
		MS+CP	0.3034				1.176		
$3_1^- \rightarrow 2_1^+$	—	MS	8.70E-7				0.0017	E1	
		MS+CP	8.70E-7				0.0017		
$3_1^- \rightarrow 2_1^+$	—	MS	0.1623				0.066	M2	
		MS+CP	0.1623				0.066		

<sup>a</sup>Cluster model with Minnesota force.

<sup>b</sup>Cluster model with Volkov force.

### 3.2. $^{21}\text{Mg}$ isotope

The energy levels of  $^{21}\text{Mg}$  are shown in Fig. 2, where the ground state and the first excited state are very well reproduced. Experimentally, there are two adjacent positive-parity levels below 2 MeV, which are  $3/2^+$  and the recently discovered [15] ( $9/2^+$ ). Those two levels appear in the results of the three model spaces, but zbme space does not give the correct ordering of them. All experimentally levels above 3 MeV, with uncertain spin

and parity appear in our calculations reasonably. The two doublet states ( $3/2^+$ ,  $5/2^+$ ) at 3.086 and 3.244 MeV, and the doublet state ( $7/2^+$ ,  $9/2^+$ ) at 3.643 MeV, appear in the calculations within the model spaces zbme, psdpf, and sd (USDC) and may be identified as  $3/2_2^+$ ,  $5/2_2^+$ , and  $9/2_2^+$ , respectively. However, the USDB and USDI interactions reverse the ordering of  $3/2_2^+$  and  $5/2_2^+$  states.

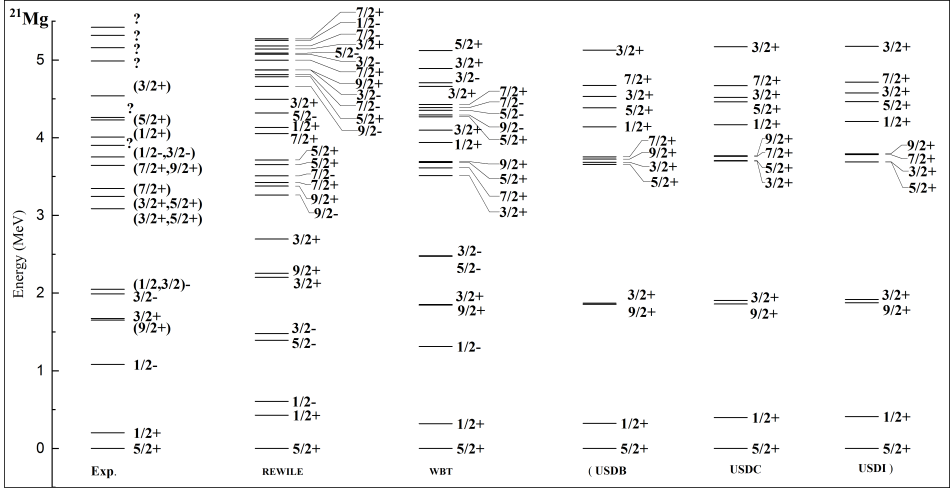


Fig. 2. The calculated and experimental level schemes for  $^{21}\text{Mg}$ . The experimental value of energy level ( $9/2^+$ ) at 1.672 MeV is taken from Ref. [15], and the other from [34].

The first excited negative-parity state in  $^{21}\text{Mg}$  is  $1/2^-$  which appears experimentally at 1.081 MeV. According to the calculations within zbme and psdpf spaces, this state appears at 0.606 and 1.313 MeV, respectively. The uncertain doublet state ( $1/2, 3/2$ ) $^-$  at 2.048 MeV adjacent to the  $3/2^-$  state at 1.989 MeV, may be the  $5/2_1^-$  state appearing close to  $3/2_1^-$  in the calculations of zbme and psdpf spaces. Also, our calculations within zbme and psdpf spaces, respectively, found  $3/2_2^-$  state at 4.871 and 4.71 MeV corresponding to the experimentally uncertain doublet ( $1/2^-, 3/2^-$ ) at 3.752 MeV.

The reduced probabilities for E2 transitions from the ground state to the excited states  $1/2_1^+$  and  $9/2_1^+$  were measured for the first time by Ruotsalainen *et al.* [15], and they obtained three different measured values of  $B(\text{E}2)$  for each transition and adopted the values 13.3(4) and 25(4) W.u. for the first and the second transition, respectively. They compared their measurements with shell model calculations using USDB interaction, as well as coupled-cluster effective interaction (CCEI), the in-medium similarity renormalization group (IM-SRG), and the symmetry-adapted no-core shell model (SA-NCSM) *ab initio* calculations which were carried out within 13 major

shells model space. The standard values of effective charges ( $\Delta e^{\pi,\nu} = 0.35 e$  and  $\Delta e^{\pi,\nu} = 0.5 e$ ) were used with USDB and CCEI only. A good overall agreement of their calculations of  $B(E2)$  and experiment, but the best was obtained by CCEI and shell model with phenomenological effective charge  $\Delta e^{\pi,\nu} = 0.35 e$ . Our calculations for the reduced transition probabilities  $B(E2)$  are displayed in Table 2. In the MS rows, the free nucleons charge values are used, and the results are reasonable as compared with their corresponding experimental values. The inclusion of core-polarization effects (MS+CP) enhances the calculations greatly, and raised the sd model space results to be equal to the experimental values. However, the calculation of  $B(E2)$  for the transition from the ground state to the excited state  $9/2^+$  within  $sd$ +CP reproduced the experimental value 22(5) W.u. (see Table I of Ref. [15], while restricting the hole states to  $1s_{1/2}$  orbit only in psdpf+CP calculation raising this  $B(E2)$  value toward the adopted one, *i.e.* 25(4).

Table 2 includes also a prediction to two  $B(M3)$  values. The effect of CP is clear in all model spaces, where the results are reduced and appear comparable for each transition.

Table 2. The calculated and the available experimental reduced transition probabilities (in W.u.) in  $^{21}\text{Mg}$ . The calculations performed within shell model space are referred as (MS) and included core polarization effects as (MS+CP).

$J_{ni}^{\pi} \rightarrow J_{nf}^{\pi}$	Exp.		zbme		sd		psdpf		$B(\varpi L)$	Other calc.
			REWILE	USDB	USDC	USDI	WBT	[15]		
$\frac{5}{2}^+ \rightarrow \frac{1}{2}^+$	13.3(4)	MS	2.532	5.276	5.209	5.214	5.085	E2	12.3 <sup>a</sup> ,9.7 <sup>b</sup>	
		MS+CP	10.29	10.31	10.22	10.22	11.56		14.6 <sup>c</sup>	
$\frac{5}{2}^+ \rightarrow \frac{9}{2}^+$	25(4)	MS	7.800	12.38	12.35	12.40	12.32	E2	24.8 <sup>a</sup> ,	
		MS+CP	11.78	21.57	21.43	21.49	24.02		17.3 <sup>b</sup> ,31 <sup>c</sup>	
$\frac{5}{2}^+ \rightarrow \frac{1}{2}^+$	—	MS	8.967	10.29	10.26	10.17	10.01	M3		
		MS+CP	6.818	5.885	5.870	5.823	6.423			
$\frac{5}{2}^+ \rightarrow \frac{9}{2}^+$	—	MS	4.430	5.762	5.501	5.386	4.992	M3		
		MS+CP	3.451	3.795	3.623	3.556	3.422			

<sup>a</sup>Calculated by CCEI ( $\Delta e^{\pi,\nu} = 0.35 e$ ).

<sup>b</sup>Calculated by IM-SRG.

<sup>c</sup>Calculated by SA-NCSM.

### 3.3. $^{22}\text{Mg}$ isotope

The experimental and theoretical level schemes of  $^{22}\text{Mg}$  nucleus are shown in Fig. 3. The sd shell model calculations are carried out through the configurations interaction of 6 nucleons (4 protons+ 2 neutrons). The three USD interactions describe the positive-parity states up to 5.5 MeV very well. Also, zbme and psdpf spaces produce those positive-parity states. However, the experimental energy value of the  $1_1^+$  state is 5.089 MeV, while it

appears at 6.205 MeV in *zbme* space (not shown in Fig. 3), and at 5.44 MeV in *psdpf* space. The first negative-parity state is  $2_1^-$  which appears at 5.09 and 5.05 MeV in the results of *zbme* and *psdpf* spaces, respectively, and corresponds to the experimental value of the  $(2^-)$  state at 5.296 MeV. The experimental energy level at 5.318 MeV has the uncertain spin assignment  $(1,2,3)$ , and the parity was unassigned. However, this level corresponds to the negative parity state  $3_1^-$ , which appears at 5.386 and 5.632 MeV in the calculations of *zbme* and *psdpf* spaces, respectively. In the PSDPF interaction calculation of Bouhelal *et al.* [21], the first  $2^-$  and  $3^-$ -states are found respectively, at 4.987 and 5.632 MeV.

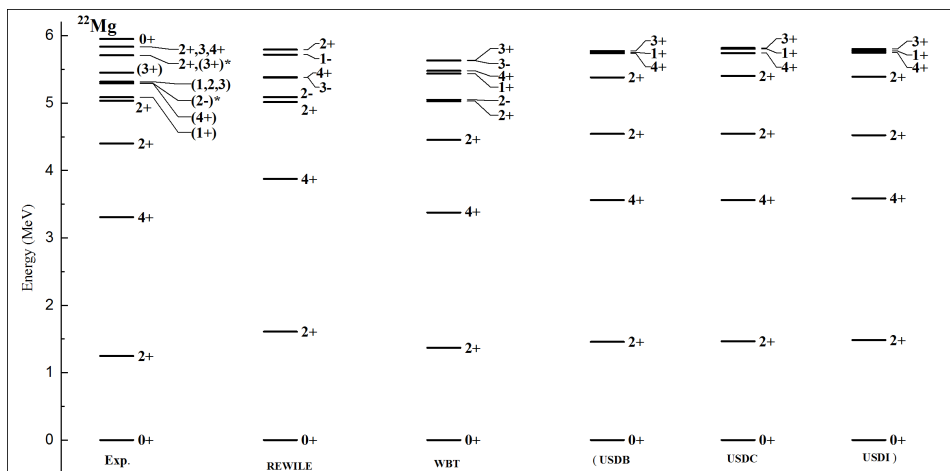


Fig. 3. The calculated and experimental level schemes for  $^{22}\text{Mg}$ . The experimental data are taken from [34].

The calculated reduced transition probabilities of  $^{22}\text{Mg}$  are given in Table 3 and compared with the available data. Model space calculations (MS) and those including core-polarization effects (MS+CP) are both listed. For  $^{22}\text{Mg}$ , the higher energy configurations necessary for CP effects are obtained through excitations of nucleons from  $1s_{1/2}$ ,  $1p_{3/2}$ ,  $1p_{1/2}$ , and  $1d_{5/2}$  orbits into higher orbits outside the model space, with  $9\hbar\omega$  excitations. The effects of CP enhance all model spaces calculations of  $B(E2)$ , and draw them to be close to the adopted experimental values. Henderson *et al.* [35] measured new value for the  $B(E2; 2_1^+ \rightarrow 0_1^+)$  in the mirror pair  $^{22}\text{Mg}-^{22}\text{Ne}$  by Coulomb excitation. Their experimental value is  $76.1_{-9.8}^{+9.2} e^2\text{fm}^4$  (20.8(26) W.u.) [35, 36] which is lower than the adopted value  $95.2_{-26.8}^{+62.4} e^2\text{fm}^4$  (26(11) W.u.) [34, 35] and more precise. They also performed two *ab initio* calculations for  $B(E2; 2_1^+ \rightarrow 0_1^+)$  without the use of effective charges, the no-core symplectic shell model (NCSpM) and IM-SRG. The NCSpM calculations found the

$B(E2)$  value equal to  $73.2\text{e}^2\text{fm}^4$  (19.95 W.u.) which agreed with their new value, while their IM-SRG calculations underpredict it. However, our sd+CP and psdpf+CP calculations for this  $B(E2)$  value found it around 28 W.u. ( $104.74\text{e}^2\text{fm}^4$ ) and 24.74 W.u. ( $90.78\text{e}^2\text{fm}^4$ ), respectively, which are in agreement with the adopted experimental value. The result of zbme+CP calculation is 17.38 W.u. ( $63.77\text{e}^2\text{fm}^4$ ) which is a reasonable value as compared with the new and the adopted  $B(E2)$ .

Table 3. The calculated and the available experimental reduced transition probabilities (in W.u.) in  $^{22}\text{Mg}$ . The calculations performed within shell model space are referred as (MS) and the ones that included core polarization effects as (MS+CP).

$J_{ni}^\pi \rightarrow J_{nf}^\pi$	Exp. [34]		zbme		sd		psdpf	$B(\varpi L)$	Other calc. [35]
			REWILE	USDB	USDC	USDI	WBT		
$2_1^+ \rightarrow 0_1^+$	26(11)	MS	3.3490	6.3010	6.2680	6.2760	6.1360	E2	19.95 <sup>a</sup>
	20.8(26)*	MS+CP	17.380	28.190	28.080	28.070	24.740		11.26 <sup>b</sup> , 9.67 <sup>c</sup>
$4_1^+ \rightarrow 2_1^+$	21(5)	MS	4.2270	6.9460	6.8790	6.8620	6.9620	E2	
		MS+CP	21.100	16.600	16.470	16.430	19.600		
$2_2^+ \rightarrow 0_1^+$	> 0.33	MS	0.1370	0.0053	0.0128	0.0170	0.0064	E2	
		MS+CP	0.9659	0.3150	0.2660	0.2440	0.2340		
$2_3^+ \rightarrow 0_1^+$	> 8.3E-5	MS	0.8050	0.8930	0.9590	0.9570	0.9840	E2	
		MS+CP	0.7790	0.8280	0.9180	0.9280	0.9490		
$2_5^+ \rightarrow 2_1^+$	0.08(5)	MS	0.3440	0.0310	0.0320	0.0240	0.0765	E2	
		MS+CP	0.1300	0.0610	0.0640	0.0850	0.0580		
$2_5^+ \rightarrow 0_1^+$	0.12(5)	MS	0.1230	0.0050	0.0130	0.0170	0.0004	E2	
		MS+CP	0.0690	0.1084	0.1429	0.1590	0.1173		
$2_2^+ \rightarrow 2_1^+$	> 0.029	MS	0.2330	0.2650	0.2710	0.2820	0.2700	M1	
		MS+CP	0.2330	0.2650	0.2710	0.2820	0.2700		
$2_3^+ \rightarrow 2_1^+$	> 5.1E-6	MS	0.2920	0.0480	0.0430	0.0430	0.0450	M1	
		MS+CP	0.2920	0.0480	0.0430	0.0430	0.0450		
$2_5^+ \rightarrow 2_1^+$	0.007(5)3	MS	0.3650	0.0040	0.0010	0.0010	0.0110	M1	
		MS+CP	0.3650	0.0040	0.0010	0.0010	0.0110		
$4_1^+ \rightarrow 2_1^+$	—	MS	0.2240	0.1503	0.1612	0.1540	0.1505	M3	
		MS+CP	0.2470	0.1604	0.1759	0.1680	0.1500		
$2_1^- \rightarrow 2_1^+$	—	MS	4.20E-3	—	—	—	2.76E-5	E1	
		MS+CP	4.20E-3	—	—	—	2.76E-5		
$2_1^- \rightarrow 2_1^+$	—	MS	1.1050	—	—	—	3.3980	E3	
		MS+CP	0.1980	—	—	—	1.1480		
$2_1^- \rightarrow 2_1^+$	—	MS	0.6820	—	—	—	0.0870	M2	
		MS+CP	0.6820	—	—	—	0.0870		

\*Taken from Ref. [35].

<sup>a</sup>Calculated by NCSpM.

<sup>b</sup>Calculated by IM-SRG (EM1.8/2.0 interaction).

<sup>c</sup>Calculated by IM-SRG (N2L0opt interaction).

On the other hand, the CP has ignorable effect on the  $B(M1)$  in  $^{22}\text{Mg}$ , and their MS results are reasonable. Also,  $B(E1)$  and  $B(M2)$  are unchanged due to introducing CP, while the values of  $B(E3)$  and  $B(M3)$  are reduced by taking CP effects into account.

### 3.4. $^{23}\text{Mg}$ isotope

Figure 4 shows the experimental and theoretical energy levels of  $^{23}\text{Mg}$ . The theoretical results are obtained by mixing the configurations within the model spaces sd, zbme, and psdpf, and diagonalizing them in the presence of the USD, REWILE and WBT interactions, respectively. The positive- and negative-parity states below 5.5 MeV are very well described. The  $(3/2)^+$  state at 2.905 MeV is very well reproduced within USD interactions, but the zbme space calculations found it at 4.41 MeV. The two doublet  $3/2^+$ ,  $5/2^+$  states that appeared experimentally at 3.86 and 5.287 MeV, respectively, are identified in our calculations as  $5/2_2^+$  and  $5/2_3^+$  states, however,  $5/2_3^+$  is missed in the USDB/C/I interactions, while  $5/2_4^+$  state is very well reproduced around 5.6 MeV.

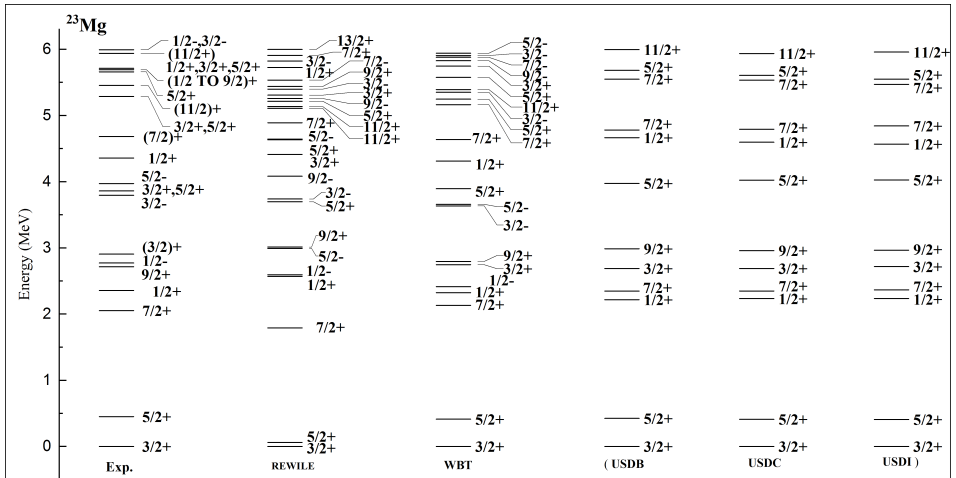


Fig. 4. The calculated and experimental level schemes for  $^{23}\text{Mg}$ . The experimental data are taken from [34].

Below 5.5 MeV, there are three experimental negative-parity states, which have spin and parity values:  $1/2^-$ ,  $3/2^-$  and  $5/2^-$ . The zbme and psdpf spaces calculations produce these states reasonably and predict the presence of other negative-parity states, as shown in Fig. 4. At the excitation energy ( $E_x \approx 6$  MeV), a level with experimentally uncertain spin and parity  $1/2^-$ ,  $3/2^-$  is found. This state is corresponding to  $3/2_3^-$  which appears at 5.821 and 5.905 MeV in the level schemes of zbme and psdpf spaces, respectively.

In Table 4, we display the reduced transition probabilities which are calculated by using the shell model wave functions for the initial and final states, and compared with the available experimental data. The role of CP effects in the enhancement of  $B(E2)$  values is very clear, as compared with the available experimental data. Similar to  $^{22}\text{Mg}$ , the effect of CP on  $B(M1)$  and  $B(E1)$  is ignorable, and their MS calculations are comparable to

Table 4. The calculated and the available experimental reduced transition probabilities (in W.u.) in  $^{23}\text{Mg}$ . The calculations performed within shell model space are referred as (MS) and that included core polarization effects as (MS+CP).

$J_{ni}^{\pi} \rightarrow J_{nf}^{\pi}$	Exp. [34]		zbme		sd		psdpf	B( $\varpi$ L)	Other calc. [37]
			REWILE	USDB	USDC	USDI	WBT		
$5/2_1^+ \rightarrow 3/2_1^+$	$24_{-13}^{+20}$	MS	4.055	9.67	9.544	9.495	9.297	E2	27.1
		MS+CP	21.84	23.22	22.96	22.84	9.297		
$7/2_1^+ \rightarrow 3/2_1^+$	$7.5_{-13}^{+18}$	MS	1.542	3.898	3.93	3.94	3.961	E2	14.7
		MS+CP	7.667	6.305	6.368	6.375	3.961		
$7/2_1^+ \rightarrow 3/2_1^+$	$6.5_{-16}^{+21}$	MS	3.173	5.171	5.19	5.19	5.47	E2	19.6
		MS+CP	6.158	6.422	6.44	6.450	6.797		
$1/2_1^+ \rightarrow 5/2_1^+$	$6.9_{-12}^{+18}$	MS	1.961	2.92	2.97	2.99	2.57	E2	9.6
		MS+CP	6.797	5.607	5.651	5.694	7.443		
$9/2_1^+ \rightarrow 5/2_1^+$	$26.5_{-30}^{+37}$	MS	3.071	6.411	6.429	6.421	6.21	E2	23.6
		MS+CP	13.43	28.38	28.37	28.30	24.51		
$5/2_1^+ \rightarrow 3/2_1^+$	0.209 (15)	MS	0.029	0.170	0.168	0.167	0.179	M1	0.049
		MS+CP	0.029	0.170	0.168	0.167	0.179		
$7/2_1^+ \rightarrow 5/2_1^+$	$0.07_{-11}^{+16}$	MS	0.023	0.127	0.127	0.128	0.141	M1	0.021
		MS+CP	0.023	0.127	0.127	0.128	0.141		
$3/2_1^- \rightarrow 1/2_1^-$	0.023(6)	MS	0.055	-	-	-	0.108	M1	
		MS+CP	0.055	-	-	-	0.108		
$3/2_1^- \rightarrow 3/2_1^+$	< 3	MS	1.756	-	-	-	0.7236	M2	
		MS+CP	1.756	-	-	-	0.7236		
$1/2_1^- \rightarrow 3/2_1^+$	-	MS	4.5E-4	-	-	-	1.09E-2	M2	
		MS+CP	4.5E-4	-	-	-	1.09E-2		
$3/2_1^- \rightarrow 5/2_1^+$	-	MS	0.0212	-	-	-	0.078	M2	
		MS+CP	0.0212	-	-	-	0.078		
$1/2_1^- \rightarrow 3/2_1^+$	$5.2\text{E-}4_{-6}^{+8}$	MS	8.2E-4	-	-	-	9E-4	E1	
		MS+CP	8.2E-4	-	-	-	9E-4		
$3/2_1^- \rightarrow 3/2_1^+$	$37\text{E-}6_{-17}^{+22}$	MS	3.1E-4	-	-	-	0.001	E1	
		MS+CP	3.1E-4	-	-	-	0.001		
$3/2_1^- \rightarrow 5/2_1^+$	$7.1\text{E-}4_{-9}^{+13}$	MS	12E-4	-	-	-	2.4E-4	E1	
		MS+CP	12E-4	-	-	-	2.4E-4		
$3/2_1^- \rightarrow 5/2_1^+$	-	MS	0.963	-	-	-	1.1E-3	E3	
		MS+CP	0.423	-	-	-	1.1E-3		
$3/2_1^- \rightarrow 3/2_1^+$	-	MS	0.649	-	-	-	0.318	E3	
		MS+CP	0.261	-	-	-	0.318		

the corresponding experimental data. The last column of Table 4 includes cluster model calculations for  $B(E2)$ , which considered the cluster structure for  $^{23}\text{Mg}$  as  $^{12}\text{C}+^{11}\text{C}$  [37]. Some cluster model results are comparable with their corresponding experimental data.

#### 4. Conclusions

The shell model with configurations interaction is applied on  $^{20-23}\text{Mg}$  isotopes to produce the positive- and negative-parity states and calculate the reduced transition probabilities between them. To achieve this task, three model spaces are used: sd, zbme, and psdpf. The universal SD interactions, USDB, USDC and USDI reproduce comparable results for the positive-parity states. In zbme space, the  $1p_{1/2}$  orbit is added to the  $2s1d$  shells, and thus the negative- as well as positive-parity states are produced. The psdpf space, is the most suitable space to produce all intruder negative-parity states in sd-shell nuclei, due to full  $1\hbar\omega$  excitations. Thus, positive- and negative-parity states in exotic  $^{20-23}\text{Mg}$  isotopes are very well reproduced by calculations achieved within zbme and psdpf spaces in the presence of Reehal–Wildenthal and WBT interactions, respectively.

In the model-dependent calculations of reduced transition probabilities, effective charge and effective  $g$ -factors are usually used. Instead of using those free parameters, we depend, in the present work, on microscopic theory without using any free parameter to calculate  $B(EL)$  and  $B(ML)$ . In core-polarization effects, intermediate particle–hole excitations are taken into account in the presence of residual interaction. The inclusion of microscopic core-polarization effects, in the presence of Modified Surface Delta Interaction (MSDI) as residual interaction, enhances the results of  $B(E2)$  and shift them closer to the experimental data. Moreover,  $B(E3)$  and  $B(M3)$  are affected by CP, while  $B(E1)$ ,  $B(M1)$ , and  $B(M2)$  are not.

#### REFERENCES

- [1] B.A. Brown, B. Wildenthal, «Strengths of transitions between  $0^+$  and  $1^+$  states and their relationship to inelastic electron scattering form factors: Example of  $^{24}\text{Mg}$ », *Phys. Rev. C* **27**, 1296 (1983).
- [2] B.J. Cole, «Large-basis shell-model calculations for», *J. Phys. G: Nucl. Phys.* **2**, 541 (1976).
- [3] W.A. Richter, B.A. Brown, « $^{26}\text{Mg}$  observables for the USDA and USDB Hamiltonians», *Phys. Rev. C* **80**, 034301 (2009).
- [4] F.H.R. M. Wiescher, J. Gorres, «Nucleosynthesis and its implications on nuclear and particle physics», in:, in «Proceeding of the NATO advanced research workshop», 1986.

- [5] IDS Collaboration (M. Lund *et al.*), «Beta-delayed proton emission from  $^{20}\text{Mg}$ », *Eur. Phys. J. A* **52**, 304 (2016).
- [6] L.J. Sun *et al.*, « $\beta$ -decay study of the  $T_z = -2$  proton-rich nucleus  $^{20}\text{Mg}$ », *Phys. Rev. C* **95**, 014314 (2017).
- [7] B.H. Wildenthal, «Empirical strengths of spin operators in nuclei», *Prog. Part. Nucl. Phys.* **11**, 5 (1984).
- [8] B.A. Brown, W.H. Richter, «New “USD” Hamiltonians for the sd shell», *Phys. Rev. C* **74**, 034315 (2006).
- [9] A. Magilligan, B.A. Brown, «New isospin-breaking “USD” Hamiltonians for the sd shell», *Phys. Rev. C* **101**, 064312 (2020).
- [10] A.A. Al-Sammarræe *et al.*, «Application of USDA and SDBA Hamiltonians in calculating the excited states of odd- $A$  magnesium isotopes», *Eur. Phys. J. Plus* **129**, 1125 (2014).
- [11] N.A. Smirnova, A. Coc, « $^{21}\text{Na}(p, \gamma)^{22}\text{Mg}$  thermonuclear rate for  $^{22}\text{Na}$  production in novæ», *Phys. Rev. C* **62**, 045803 (2000).
- [12] A.S.J. Murphy *et al.*, «Level structure of  $^{21}\text{Mg}$ : Nuclear and astrophysical implications», *Phys. Rev. C* **73**, 034320 (2006).
- [13] A.T. Gallant *et al.*, «Breakdown of the Isobaric Multiplet Mass Equation for the  $A = 20$  and  $21$  Multiplets», *Phys. Rev. Lett.* **113**, 082501 (2014).
- [14] D.T. Yordanov *et al.*, «Spin and magnetic moment of  $^{23}\text{Mg}$ », *J. Phys. G: Nucl. Part. Phys.* **44**, 075104 (2017).
- [15] P. Ruotsalainen *et al.*, «Isospin symmetry in  $B(E2)$  values: Coulomb excitation study of  $^{21}\text{Mg}$ », *Phys. Rev. C* **99**, 051301 (2019).
- [16] J.S. Randhawa *et al.*, «Observation of excited states in  $^{20}\text{Mg}$  sheds light on nuclear forces and shell evolution», *Phys. Rev. C* **99**, 021301 (2019).
- [17] B. Longfellow *et al.*, «Two-neutron knockout as a probe of the composition of states in  $^{22}\text{Mg}$ ,  $^{23}\text{Al}$ , and  $^{24}\text{Si}$ », *Phys. Rev. C* **101**, 031303 (2020).
- [18] C.A. Diget *et al.*, «Structure of excited states in  $^{21}\text{Mg}$  studied in one-neutron knockout», *Phys. Rev. C* **77**, 064309 (2008).
- [19] E.K. Warburton, B.A. Brown, «Effective interactions for the  $0p1s0d$  nuclear shell-model space», *Phys. Rev. C* **46**, 923 (1992).
- [20] M. Bouhelal *et al.*, «A PSDPF interaction to describe the  $1\hbar\omega$  intruder states in sd shell nuclei», *Nucl. Phys. A* **864**, 113 (2011).
- [21] M. Bouhelal, F. Haas, E. Caurier, F. Nowacki, «Shell-model studies of  $^{22}\text{Mg}$  at excitations of interest for the thermonuclear radiative capture reactions» *PoS NIC-XIII*, 074 (2014).
- [22] A.A. Al-Sammarræie, F.A. Ahmed, A.A. Okhunov, «Large Scale Shell Model Calculations of the Negative-parity States Structure in Nucleus», *Ukrainian J. Phys.* **66**, 293 (2021).
- [23] A.A. Al-Sa, A.A. Abbass, «Core-Polarization Effects on the Isovector Magnetic Dipole Transitions in  $^{24}\text{Mg}$ », *Chinese J. Phys.* **50**, 768 (2012).

- [24] R.A. Radhi, N.T. Khalaf, A.A. Najim, «Elastic magnetic electron scattering from  $^{17}\text{O}$ ,  $^{25}\text{Mg}$  and  $^{27}\text{Al}$ », *Nucl. Phys. A* **724**, 333 (2003).
- [25] R.A. Radhi, «Coulomb excitations of open-shell nuclei», *J. Phys. A* **42**, 214047 (2009).
- [26] B.S. Reehal, B.H. Wildenthal, «Shell-model calculation for masses 15, 16, and 17», *Particles Nucl.* **6**, 137 (1973)
- [27] T.W. Donnelly, I. Sick, «Elastic magnetic electron scattering from nuclei», *Rev. Mod. Phys.* **56**, 461 (1984).
- [28] P.J. Brussaard, P.W.M. Glaudemans, «Shell-Model Applications in Nuclear Spectroscopy», *North-Holland Publishing Company*, 1977.
- [29] J. Suhonen, «From Nucleons to Nucleus: Concepts of Microscopic Nuclear Theory», *Springer, Berlin, Heidelberg* 2007.
- [30] B.A. Brown *et al.*, «Oxbash for Windows PC», MSU-NSCL Report No. 1289, 2004.
- [31] P. Descouvemont, «Microscopic three-cluster study of  $^{20}\text{O}$ ,  $^{20}\text{Mg}$  and  $^{19}\text{N}$ ,  $^{19}\text{Mg}$  exotic nuclei», *Phys. Lett. B* **437**, 7 (1998).
- [32] J.D. Holt, J. Menéndez, A. Schwenk, «Three-Body Forces and Proton-Rich Nuclei», *Phys. Rev. Lett.* **110**, 022502 (2013).
- [33] N. Michel, J.G. Li, F.R. Xu, W. Zuo, «Description of proton-rich nuclei in the  $A \approx 20$  region within the Gamow shell model», *Phys. Rev. C* **100**, 064303 (2019).
- [34] National Nuclear Data Center, «International network of nuclear structure and decay data evaluators», <https://www.nndc.bnl.gov>
- [35] J. Henderson *et al.*, «Testing microscopically derived descriptions of nuclear collectivity: Coulomb excitation of  $^{22}\text{Mg}$ », *Phys. Lett. B* **782**, 468 (2018).
- [36] M. Wiedeking, A.O. Macchiavelli, «Global trends of nuclear  $d_{5/2}^{2,3,4}$  configurations», *Eur. Phys. J. A* **56**, 1 (2020).
- [37] A. Kabir, B. Buck, «Cluster model of  $^{23}\text{Na}$  and  $^{23}\text{Mg}$ », *Nucl. Phys. A* **518**, 449 (1990).